G^0 Electronics and Data Acquisition (Forward-Angle Measurements)

D. Marchand, J. Arvieux, L. Bimbot, A. Biselli, J. Bouvier, H. Breuer, R. Clark, J.-C. Cuzon, M. Engrand, R. Foglio, et al.

G⁰ Electronics and Data Acquisition (Forward-Angle Measurements)

D. Marchand, [b] J. Arvieux, [b] G. Batigne, [c] L. Bimbot, [b]
A. Biselli, [a] J. Bouvier, [c] H. Breuer, [e] R. Clark, [a] J.-C. Cuzon, [b]
M. Engrand, [b] R. Foglio, [c] C. Furget, [c] X. Grave, [b] B. Guillon, [c]
H. Guler, [b] P.M. King, [e,d] S. Kox, [c] J. Kuhn, [a] Y. Ky, [b]
J. Lachniet, [a] J. Lenoble, [b] E. Liatard, [c] J. Liu, [e] E. Munoz, [c]
J. Pouxe, [c] G. Quéméner, [c] B. Quinn, [a] J.-S. Réal, [c]
O. Rossetto, [c] R. Sellem, [b]

[a]*Department of Physics, Carnegie Mellon University, Pittsburgh, PA 15213, USA*

[b]*Institut de Physique Nucléaire d'Orsay (UMR8608), CNRS/IN2P3, Université Paris Sud, Orsay, France*

[c]*LPSC, Université Joseph Fourier Grenoble 1, CNRS/IN2P3, Institut National Polytechnique de Grenoble, Grenoble, France*

[d]*Loomis Laboratory of Physics, University of Illinois, Urbana IL 61801, USA*

[e]*Department of Physics, University of Maryland, College Park, MD 20472, USA*

Abstract

The G⁰ parity-violation experiment at Jefferson Lab (Newport News, VA) is designed to determine the contribution of strange/anti-strange quark pairs to the intrinsic properties of the proton. In the forward-angle part of the experiment, the asymmetry in the cross section was measured for $\vec{e}p$ elastic scattering by counting the recoil protons corresponding to the two beam-helicity states. Due to the high accuracy required on the asymmetry, the G⁰ experiment was based on a custom experimental setup with its own associated electronics and data acquisition (DAQ) system. Highly specialized time-encoding electronics provided time-of-flight spectra for each detector for each helicity state. More conventional electronics was used for monitoring (mainly FastBus). The time-encoding electronics and the DAQ system have been designed to handle events at a mean rate of 2 MHz per detector with low deadtime and to minimize helicity-correlated systematic errors. In this paper, we outline the general architecture and the main features of the electronics and the DAQ system dedicated to G⁰ forward-angle measurements.

Key words: parity violation, electron scattering, time encoding, high rate electronics

1 Introduction

The G^0 parity-violation experiment described in references [1] and [2] was performed in hall C at the Jefferson Laboratory (Newport News, VA). The goal of this experiment was to measure the strangeness content of the nucleon, determining the strange electric and magnetic form factors of the proton. Combining forward- and backward-angle measurements (Rosenbluth separation), the G^0 experiment will be able to separate the strange electric form factor from the strange magnetic one for specific Q^2 values (at least Q^2=0.23 $(\mathrm{GeV}/c)^2$ and Q^2=0.64 $(\mathrm{GeV}/c)^2$). The first data-taking performed in 2004 was dedicated to forward-angle measurements which determined a linear combination of the strange electric and magnetic form factors for each of eighteen Q^2-bins, extending from 0.1 to 1.0 $(\mathrm{GeV}/c)^2$. The results, published in reference [3], indicate nonzero, Q^2-dependent, strange-quark contributions to the charge and/or current densities of the proton. In the forward-angle mode, measurements were made of the counting rate asymmetry for recoil protons from the elastic scattering of longitudinally polarized electrons from unpolarized protons. This asymmetry, arising from the parity violation property of the weak interaction (Z^0 boson exchange), is of the order of 10^{-6} to 10^{-5} within the Q^2 range of interest. Measuring such small asymmetries required counting statistics of the order of 10^{13} events which led to specific requirements such as a high intensity electron beam, a thick, high-power LH_2 target, a large acceptance detector system including a spectrometer and a dedicated electronics system allowing time-of-flight measurements to isolate elastic scattering from inelastic processes. The requisite data rate excluded the possibility of event-by-event readout, necessitating spectrometer optics which separate the elastic events without the use of tracking detectors. As the angles of elastically scattered electrons are very close to the incident beam ($7°$ to $21°$), it was preferable to detect the recoil protons between $52°$ and $76°$.

The G^0 experimental setup was designed to be used for both forward- and backward-angle measurements. The backward-angle measurements, performed in 2006-2007, required the rotation of the spectrometer by $180°$ and the addition of various detectors (scintillators and Cerenkov counters) in order to detect scattered electrons from large angle $\vec{e}p$ elastic scattering and quasi-elastic electron-deuteron scattering. A description of the experimental setup for backward-angle measurements including its specific electronics can be found in reference [2].

For the forward-angle measurements, a brief description of the experimental

apparatus and the requirements of the G^0 beam structure are given in the next section. A description of the data acquisition and the trigger systems is presented in section 3. The electronics, consisting of a monitoring system (FastBus) and time-encoding electronics, is outlined in section 4 while the details of the two time-encoding sub-systems are given in sections 5 and 6.

2   G^0 Experiment for Forward-Angle Measurements

2.1   Overview

The forward-angle part of the G^0 experiment measured asymmetries in $\vec{e}p$ elastic scattering by detecting the recoil protons. As illustrated in figure 1, a longitudinally polarized 3 GeV electron beam struck a liquid hydrogen target located on the axis of a toroidal superconducting magnet. Recoil elastic/inelastic protons and other positively charged particles are deflected by the magnetic field to focal plane detectors grouped into eight sectors (referred to as octants). Each sector is instrumented by 16 pairs (two layers) of plastic scintillators. The identification of recoil elastic protons relies on time-of-flight measurements relative to the beam pulse arrival time in the target. This required a custom pulsed beam structure to provide a start time, rather than the nominal continuous beam.

2.2   Electron Beam

To allow time-of-flight measurements, for forward angle G^0 running, the beam had a specialized time structure of 31.1875 MHz, 1/16 of the standard beam pulse frequency of 499 MHz provided to each of the three halls. Therefore electron beam pulses were delivered with a period of approximately 32 ns to Hall C at an average beam current of 40 μA. With this beam structure, each pulse must carry 16 times more electrons than for the same average current in 499 MHz operation.

Effects due to the 60 Hz line frequency were averaged out by choosing a data-taking period of $\frac{1}{30}$ second (referred to as one MacroPulSe, or MPS). No data were taken during an additional period of 500 μs following each MPS. At the beginning of this period the helicity of the beam was reversed, if required, and the remainder of the period allowed time for signals to stabilize.

The macropulses were grouped into quartets. Within each quartet the helicities of the four consecutive macropulses followed one of the two allowed patterns,
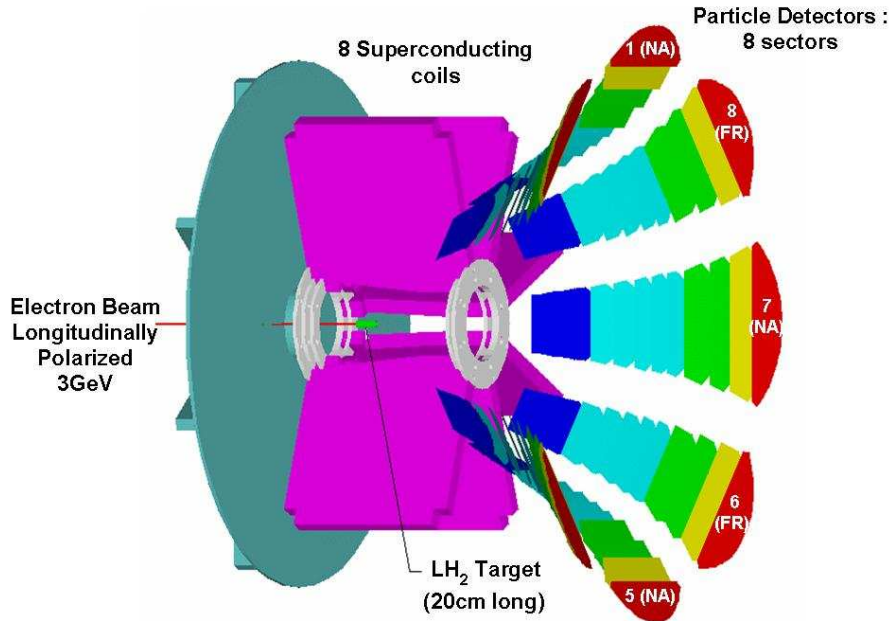
3

Fig. 1. The G^0 experimental setup dedicated to forward-angle measurements. It consists of a 20 cm liquid hydrogen target and a toroidal Superconducting Magnet System (SMS) followed by 128 pairs (front and back) of plastic scintillators grouped into eight sectors (octants). Odd numbered octants have been built by the North American (NA) part of the collaboration and the even numbered octants by the French (FR) part. Two of the superconducting coils and one octant have been removed for clarity.

either $+--+$ or $-++-$. The choice of which pattern to use for a particular quartet was made pseudo-randomly to prevent any long-term periodicity of the helicity sequence. These patterns reduce sensitivity to any linear drifts within a quartet and also ensure that asymmetry determinations can be made quartet-by-quartet. The MPS signal was sent to all sub-systems through the "trigger supervisor" described in section 3. The helicity sequence for each quartet was buffered at the source and reported to the experiment only after a delay of two quartets. This precaution prevented the helicity-related signals from having any influence on the electronics which might otherwise induce a false asymmetry.

A custom-built system [4] provided a very stable beam-arrival signal, phase-locked to a 1497 MHz resonance cavity installed just upstream of the G^0 target. This signal (referred to as Y_0) served as the start signal for the time-of-flight measurements and was sent to both time-encoding electronics sub-systems and to the monitoring system (FastBus) as described in section 4. Time-of-flight measurements were made relative to Y_0, thus avoiding the possibility of introducing a helicity-dependent bias to the time-of-flight measurements due to helicity-dependent transit time of the beam through the accelerator. A system-

atic shift of the order of ten femto-seconds could introduce an unacceptable false asymmetry. Time-of-flight measurements with respect to beam-arrival time eliminated that dependence on transit time.

While the 1497 MHz R.F. signal from the resonance cavity provides an accurate reference to phase-lock the Y_0 signal, the 48-fold ambiguity in the time of the Y_0 was resolved using a 31.1875 MHz oscillator phase-locked to the signal from a stripline beam pickup located near the cavity. The latter signal was used to reproducibly select a unique phase of Y_0 with respect to the 1497 MHz cavity signal. The response time for the signals to accommodate to a change in beam timing was 100 μs. Thus, a possible transit time shift due to beam-helicity reversal would have been accommodated during the helicity-stabilization period before resumption of data-taking.

2.3 Apparatus

The 20 cm long G^0 liquid hydrogen target was designed to minimize density fluctuations with up to 250 Watts of beam power deposited in the target. The target could be removed from the beam for diagnosis purposes. Details on the design and performances of the target can be found in references [2], [5] and [6]. This target was also used for backward-angle measurements with liquid Hydrogen and Deuterium.

Detection of scattered particles was based on a superconducting magnetic spectrometer [7,2] (referred to as SMS, figure 1). It focused elastic recoil protons through collimators onto a Q^2-segmented Focal Plane Detector array (plastic scintillators). The toroidal superconducting magnet of the spectrometer is composed of eight superconducting coils surrounding the beam axis. These coils split the detector system into octants. The SMS cryostat has a mean diameter of about 4 m and an axial length of 2 m. The magnetic field integral is $\int Bdl \approx$1.6 T·m. The angular deflection in the magnetic field ranges from 35° to 87°. The azimuthal acceptance of each octant, about 22°, was accurately defined by horizontal collimators. Vertical collimators limited the polar-angle acceptance to that corresponding to elastic scattering over the Q^2 range of interest, reducing counting rates from background. The resulting total solid angle was 0.9 sr.

The SMS was designed such that elastic recoil protons having the same momentum are focused at the same point in the focal plane independently of the interaction point in the target along the beam axis.

Each octant was instrumented with 16 Focal Plane Detectors (FPDs), each consisting of two layers made of plastic scintillator paddles (Bicron BC408) shaped and segmented to detect elastic protons corresponding to narrow bands

of Q^2. The FPDs in each octant were numbered sequentially, with the first FPD the closest to the electron beam line and the sixteenth the farthest one out. This is also the direction of increase for the Q^2 bins until a turn-around point located at detector 15. The detector system was designed such that each of the first 13 FPDs corresponds to a specific Q^2 bin. The next two FPDs (14 and 15), due to the optics of the spectrometer covered a larger Q^2 range, because of the kinematic turn-around point. The last FPD (detector 16) by design did not observe any elastic events and was used for background studies.

The construction of the detectors was shared between the North American (NA) and the French (FR) parts of the collaboration so that each part built four octants with its associated time-encoding electronics. As shown in figure 1, the NA and FR octants were mounted alternately around the beam axis to maximize azimuthal symmetry. The two-layer scintillator paddle pair of an FPD, referred to as the front and the back scintillators, were separated by a 3 mm thick sheet of polycarbonate (NA) or Aluminum (FR). These sheets reduced the rate of background coincidences caused by interactions in one scintillator producing secondaries which enter the other. Each end of each scintillator paddle was connected to a Photomultiplier Tube (PMT) through a light guide. The NA FPDs used Photonis XP2262B 12-stage PMTs with custom-built Zener-diode bases while the FR FPDs use Photonis XP2282B 8-stage PMTs with actively stabilized custom-made bases. To increase the PMT life-time, the PMTs were run at low gain and the signals were amplified. The FR bases include a pre-amplifier providing an amplification factor of 20. The amplification factor for the NA tubes was 25, provided by modified commercial PMT amplifiers.

To reduce background, particle detection was based on front-back coincidences in the two scintillator layers of each FPD. Particle identification (separation of recoil elastic protons from inelastic protons and pions) relied upon Time-of-Flight (ToF) measurements. The ToF spectra were accumulated by highly specialized time-encoding electronics described in section 4. For cross-checking purposes and to control systematic errors, the G^0 experiment benefits from two different designs of time-encoding electronics: one associated with the four NA octants and the other associated to the four FR octants. Thus, each set of data provided an independent complete measurement. The two results could be checked for consistency before being combined into the final result for the entire set of octants. In addition to the custom time-encoding electronics, conventional FastBus electronics (ADCs and TDCs) were used to acquire and store complete event-by-event data for a small fraction of beam pulses (less than 0.01%).

3 Data Acquisition System

The G^0 data acquisition was driven by the CODA (CEBAF On-line Data Acquisition) [8] system developed at JLab. The triggering and the event control were performed by the Trigger Supervisor module linked to each subsystem/crate using Trigger Interface modules. The Trigger Supervisor served as the interface between the experiment-specific triggering and the data acquisition system. The different trigger sources were input to the Trigger Supervisor. A schematic of the G^0 Data Acquisition system is presented in figure 2.
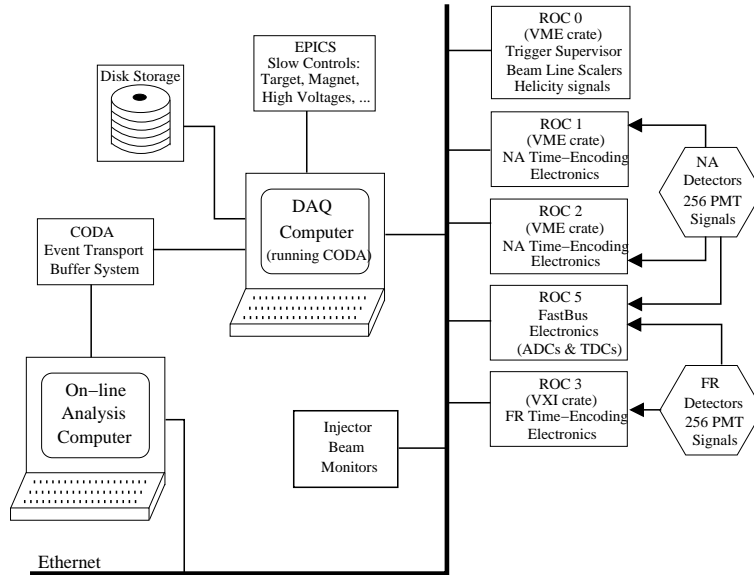

Fig. 2. Schematic of the G^0 Data Acquisition system. ROC stands for Read-Out Controller.

During production runs, the data readout of both time-encoding sub-systems was performed at the MPS rate (roughly 30 Hz). At the end of each MPS, during the "helicity-stabilization" period, the data were stored in memory buffers to allow them to be read out during the next MPS. After each MPS, the beam parameters and the data from each time-encoding sub-system were first transferred to a Read Out Controller (ROC) and then gathered with the other ROCs as a single event by the "Event Builder" in the DAQ computer. For the specialized time-encoding electronics, time-of-flight spectra corresponding to each MPS were stored. This allows an off-line cut on the data quality for each MPS before calculating asymmetries quartet by quartet.

In order to detect any possible 60 Hz noise, an "over-sampling" running mode at 120 Hz was performed occasionally. In this running mode, the NA Time-Encoding Electronics (TEE) were stored and read out four times during each MPS, once after each 1/120 of a second. The French TEE were still read out at 30 Hz, after each MPS. For the French TEE, the subdivision of the data

into subsets collected in four sub-periods of the MPS was made by means of the front-end Digital Signal Processors of each mother board. During 120 Hz acquisition, only TEE and beam parameter scalers were read out. A Fourier analysis of the 120 Hz data (ToF spectra, positions and angles of the beam, beam charge) performed after each 120 Hz run determined that the specifications regarding 60 Hz noise have been achieved.

The readout of the FastBus data (monitor events) was triggered by a prescaled copy of the Y_0 signal. This was first prescaled in hardware to provide an input rate of about 500 kHz. For typical running conditions, the rate was then reduced to 100-200 Hz by applying a software prescale factor within the trigger supervisor. More details on the G^0 trigger system can be found in reference [2].

Another set of slow control data was also recorded to control and monitor the experimental apparatus. These events contain information such as detector high voltages, beam characteristics (charge, positions, ...), target and SMS parameters.

4   Electronics

At a mean rate of 2 MHz per detector, it is impossible to store full event-by-event information (timing and amplitude of the PMT signals). Instead, it was chosen to accumulate, in hardware, histograms of the time-of-flight information provided by the time-encoding electronics. For each FPD the mean arrival time is stored for complete events, which have a front-back coincidence. No information is stored using the TEE concerning, for example, time differences between signals from the two PMTs of one scintillator. In order to monitor such detector information, conventional FastBus electronics is used to store full event information for a few beam pulses out of every 10^5. Figure 3 summarizes the whole electronics chain from PMT signals to full-event buffers.

4.1   Monitoring system

The monitor electronics consists of FastBus ADCs (LeCroy 1885F) and TDCs (LeCroy 1875A). After passing through about 36 m of RG58 cable in the experimental hall, the PMT signals were carried up to the electronics/DAQ area on 107 m of RG8 cable. In the electronics area, the design allows all signals to go to the TEE but also presents them to the FastBus monitor electronics so a small subset can be sampled on an event-by-event basis. Splitter modules route part of the PMT signal to FastBus ADCs while the other part of the signal
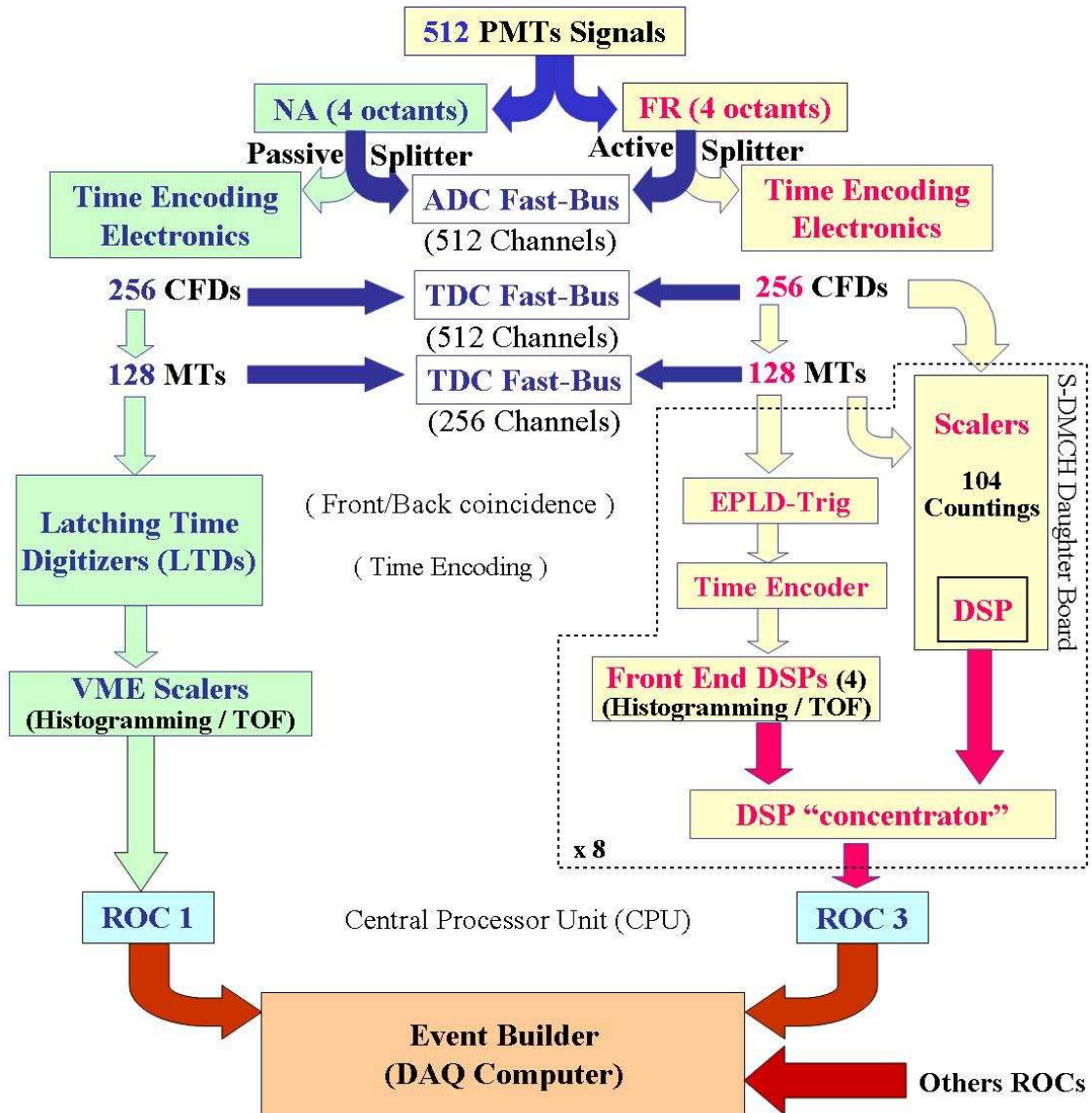
Fig. 3. General scheme of the G^0 electronics chain from PMT signals to full-event buffers.

goes to the Constant Fraction Discriminators (CFDs) which are the front-end of the TEE. The French PMT signals enter active splitters (gain 1) so that the signal sent to the TEE remains unchanged and the signal sent to FastBus ADCs is a copy of the original signal. The North American PMT signals enter passive impedance-matching 2:1 splitters which send the smaller fraction of the signal to FastBus ADCs. The larger fraction of the split signal goes to the input of commercial CFD modules. In order to achieve good time resolution, the two CFD signals from each scintillator are meantimed in hardware in each TEE sub-system. Copies of the CFD and MeanTimer (MT) outputs are also routed to FastBus TDCs. For an arbitrarily selected set of beam pulses, the

ADCs were gated and the TDCs were started and all resulting FastBus information was read out. The combination of ADC and TDC information provides full event-by-event information for this small subset of events. These FastBus events allow the study of correlations (in pulse size and/or in time) for individual detectors and for relationships between detectors. The stored FastBus events are used to study the behavior of the meantimers, to measure timing resolution, to monitor singles rates, to measure attenuation in the scintillators, and to perform other checks of the apparatus. Some of the measured quantities, such as rates of single-, double-, or triple-PMT coincidences are also used to quantify deadtime corrections to apply to the TEE data. For some low-luminosity calibration runs a fast-clear signal to all ADCs and TDCs was used to discard those FastBus events for which the CFD pattern indicated the lack of any charged particles of interest in the detectors.

4.2   Time-Encoding Electronics

The challenge in the design of the TEE is to accept all the four-fold coincidence events (complete events, requiring both PMTs for both front and back scintillators) at a mean rate of 2 MHz per detector and to accomplish the time-of-flight measurement and the subsequent histogramming. For cross-checking purposes, the G^0 experiment benefits from two different designs for TEE. The NA electronics, designed by Carnegie Mellon University (Pittsburgh, PA), is mostly based on modular electronics units whereas the French electronics, designed by IPN Orsay, is fully integrated. The advantage of such divergent paths was that there was little likelihood that both techniques would be susceptible to the same systematic errors.

Both time-encoding sub-systems are based on similar objectives in processing the front-end signals. After passing through the splitters, the PMT signals are first sent to Constant Fraction Discriminators (CFDs) to reject low energy background. Since offline walk corrections are prohibited by the lack of event-by-event data, CFDs have been chosen to provide good time resolution over a large dynamic range as the firing time is, in principle, independent of the amplitude of the input signal. Then, to achieve good time resolution, the timing signals from opposite ends of each scintillator are meantimed in hardware. This ensures that the encoded time is almost independent of the hit location on the scintillator paddles. The MT signals are provided to a logic device which makes the coincidence between the front and the back scintillator signals. The timing of the coincidence events is encoded by time digitizers relative to the Y_0 signal, to determine the time-of-flight. Finally, according to their timing, each coincidence event increments the corresponding time bin in a time-of-flight spectrum built by means of VME scalers (NA) or digital signal processors (FR).

The two electronics designs include common features to control and monitor the dead time. In order to make dead time more deterministic, Next Pulse Neutralization (NPN) is enforced, meaning that encoding is disabled during the next beam pulse after a coincidence event occurs. Another feature which has been implemented in both sub-systems is the so-called "buddy" system which is used mostly as an alert to monitor beam charge fluctuation and detect any helicity dependence of dead time. In this context, similar detectors (symmetric to each other at 180° w.r.t. the beam axis) have been paired as "buddies" and separate count is kept of hits occurring on a detector while the electronics of its buddy detector are busy. Missed events due to dead time may be expected to scale like these "buddy" events. Besides the "buddy" system, the French electronics provides time-of-flight spectra of "buddy" events (referred to as "differential buddy") which takes into account the NPN. More details on the differential buddy method and its outcomes can be found in reference [9].

The characteristics of each of the two time-encoding sub-systems are given in the next two sections.

5 North-American Time-Encoding Electronics

5.1 Overview

The electronics which was developed to read out the 'North-American' octants was based on a highly modular approach using the simplest design consistent with the requirement of encoding time-of-flight spectra at rates averaging about 2 MHz per detector.

Discrimination and meantiming are performed in separate modules. The resulting meantimed signals for each front scintillator and the corresponding back scintillator are then presented to the time-encoding board, called a Latching Time Digitizer (LTD). The LTD demands a front-back coincidence and, if it is present, encodes the time-of-flight of the front meantimer as a bit pattern, as described in section 5.2.2. The bit patterns for all beam pulses within an MPS are then accumulated in channels of scaler modules at instantaneous rates up to 15.6 MHz. The main role of the LTD is to encode time-of-flight as scaler channels. At the end of an MPS, the accumulated scalers contain the information needed to construct the time spectrum. As described below, the time spectra accumulated during one MPS can be rapidly captured, allowing accumulation of the time spectra for the next MPS to begin while the spectra from the earlier MPS are being read out by the DAQ.

In addition to the series of modules through which pulses pass to be encoded as time spectra, a set of auxiliary modules are needed to generate clock trains to the LTDs. These auxiliary modules provide synchronization and time reference to the LTDs.

5.2 Signal Processing

When the PMT signals enter the electronics area the passive 2:1 splitter, discussed in section 4.1, sends the larger output signal to a LeCroy 3420 Constant Fraction Discriminator. At the high rates characteristic of this experiment, it was found that care was needed to avoid unacceptable loss of data due to the effect of sub-threshold signals distorting the pulse shape for above-threshold events. This effect was resolved by careful choice of the internal delay and fraction parameters of the CFD. As indicated in figure 3, the differential ECL output signal of the CFD was passively split to go to a meantimer and to a FastBus TDC (LeCroy 1875A) to be sampled event-by-event for monitoring purposes.

Hardware meantiming was used to render the time of the signals relatively insensitive to the position along the length of the scintillator at which the proton crossed. Custom meantimers were constructed at Carnegie Mellon University based on a meantiming ASIC (Application-Specific Integrated Circuit) developed at LPSC-Grenoble [10]. This ASIC is based on two shift-register pipelines which clock the incoming PMT signals in opposite directions. The meantime output fires when two signals overlap at the same position in the two counter-propagating pipelines. This simple principle of operation avoids recovery effects, such as long deadtime or time distortion, which are sometimes encountered in other meantimer designs. The operations performed by the meantimer board are represented schematically in figure 4. Features added by the meantimer board include reduction of accidental overlap of unrelated pulses by replacing the input pulses from the CFD with short one-shot pulses of about 2 ns fed into the meantimer ASIC. The meantimed output pulses also go through a pair of consecutive one-shots to allow separate selection of meantimer output pulse width and deadtime, subject only to the constraint that the deadtime exceed this output width. The outputs from the first of these one-shots were sent to FastBus TDCs (LeCroy 1875A) for event-by-event monitoring. The narrower pulse from the second one-shot was sent to the LTDs to form the front-back coincidence. The meantimer boards also provided temperature monitoring and compensation for shifts in clocking speed of the ASIC with temperature.
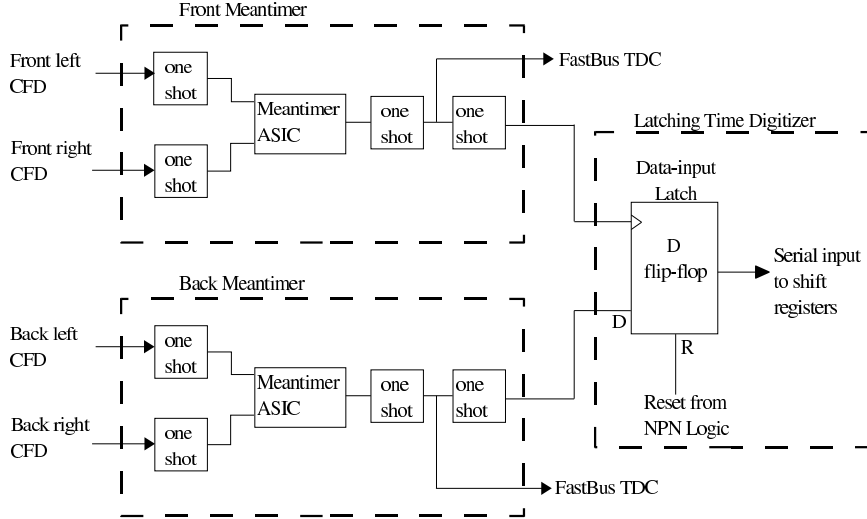
12

Fig. 4. A schematic representation of the path for NA detector signals (from a single FPD) through the meantimer modules and into the data-input latch of the LTD. The wedge on the D flip-flop indicates the Clock input while letters mark the inputs for Data and Reset.

5.2.1 Clock Gating and Distribution

The NA time-encoding modules, described in the next section, use externally-generated clock trains as the basis for their time measurements. Generation of clock trains for accurate time-of-flight measurements is based on two signals synchronized to beam arrival at the target. These signals are labeled as CLK and Y_0 in figure 5. CLK has a frequency of 499 MHz, while Y_0 (as described in section 2.2) has a frequency of 31.1875 MHz, the frequency of the beam pulses. The CLK signal (like the Y_0) is phase-locked to the arrival time of the pulses at the target rather than being aligned relative to the accelerator's R.F. or to the injection. CLK is generated from the JLab 499 MHz master oscillator signal by phase-shifting it to align with Y_0.

Figure 5 illustrates how the CLK and Y_0 are used in a custom clock-gating board to produce trains of 12 clock pulses (with the period of the 499 MHz CLK pulses). The clock-gating board simply gates off four CLK pulses with a gate synchronized to Y_0. The width of the gate and its offset relative to Y_0 are adjustable by on-board switches to compensate for cable delay variations.

A synchronization pulse, SYNC, is also generated by the clock-gating board between clock trains. The clock train and SYNC are distributed by twinax cable to custom 9-fold signal duplication boards and then fanned out, on the same type of cable, to the LTD boards. Both signals are distributed as complementary ECL to improve noise immunity.
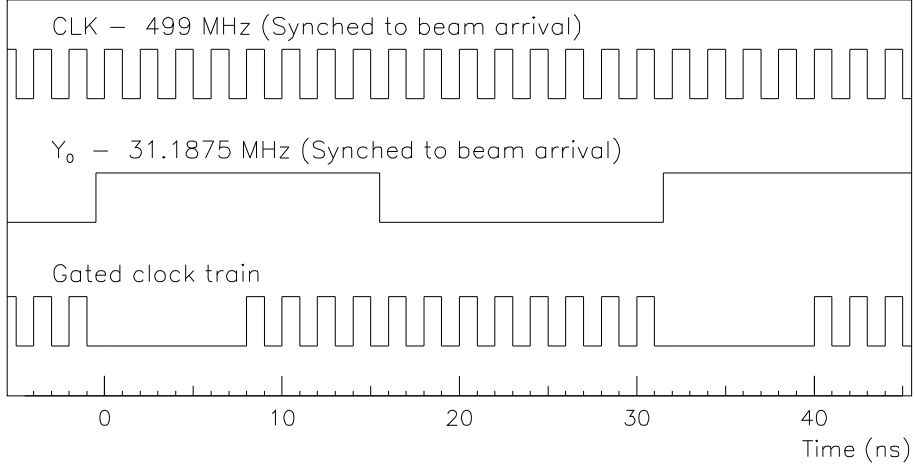
13

Fig. 5. Timing diagram showing clock trains generated based on the CLK and Y_0 signals described in the text.

5.2.2 Time Encoding Module

The time-encoding boards (LTDs) enforce the requirement of a front-back coincidence between the scintillators. As indicated schematically in figure 4, a D flip-flop is clocked by the front scintillator meantime while the meantimer pulse for the back scintillator is presented to the D input. Thus the time at which this data-input latch is set is determined by the front scintillator while the tolerance of the coincidence is set by the width of the pulse for the back meantimer, which was set to 10 ns.

The principle of operation of the LTDs provides a very simple method of accumulating time spectra for data rates of several MHz. In fact the LTD boards were tested successfully with rates of several tens of MHz. The time-encoding behaved as expected even at those rates and deadtime corrections were correctly predicted although deadtime corrections began to become large, as expected. No measurable shift of the edges of the time bins was observed for pulsed data rates ranging from a few kHz to 31.1875 MHz. An upper limit on such variation was set at a few ps per MHz.

As described below, the LTDs work by encoding each time spectrum as a simple pattern of 24 bits which can then be presented to scaler inputs. The scalers accumulate the bit patterns and thus store information from which a time spectrum can be easily unfolded. Only this spectrum is stored, so all correlations within one event are lost. The bit pattern is generated by presenting the output of the data-input latch to the serial input of a previously-cleared shift register. The shift register is clocked by the gated clock train described above and shown in figure 5. If the data-input latch is set during any clock train, a series of "ones" will be clocked into the shift register. Earlier

14

hits within a clock train will result in a longer train of "ones" being clocked in. Since the data-input latch is not reset until after the end of the clock train, the data clocked into the shift register will have a very simple format with a single zero-to-one transition encoding the time of the hit. Every 32 ns, after each clock train, the parallel outputs of the shift register are strobed to latches which present them to scaler inputs. The scalers are separate VME modules whose differential inputs are driven via twisted pair ribbon cables driven by these latches. During the period between clock trains the shift registers are also reset. The strobe of the latch and the reset of the shift registers are timed relative to the last pulse of the clock trains. The SYNC signal, which arrives in the period between clock trains, is used to detect and reset any loss of synchronization which might occur if a clock train were incorrectly gated or if the electronics made an error in counting the pulses in the clock train. The reset of the data-input latch is described below.

Finer time resolution is achieved by presenting each data-input latch to two parallel shift registers, one of which is clocked by the leading edges of the gated clock train while the other is clocked by the trailing edges. One or the other of the two shift registers is thus clocked each nano-second during the clock train. Treating the two parallel shift registers as a single inter-leaved sequence of 24 bits, the position of the zero-to-one transition then encodes the time of the data with a time bin of 1 ns. Differences between sequential bits will then be non-zero only for the time bin in which the hit occurs. Similarly, after these bit patterns have been accumulated in scalers, differences between sequential scaler channels (arranged in the order of sequential bits) represent the total number of hits which occurred in the corresponding 1 ns time bin in all clock trains for which data were accumulated. Time spectra can thus be determined, for each MPS, with the scaler values being read out only after each MPS. The scaler-channel differences span a 23 ns range of the 32 ns between beam pulses. This yields a TOF spectrum covering a 23 ns period of interest, with 1 ns time resolution. The 24th bin keeps count of events which occur in the several nano-seconds between the reset of the data-input latch and the beginning of the next clock train.

5.2.3   Scalers and DAQ Interface

The scalers that capture the time spectra are custom-built 32-channel VME scaler boards which were designed by LPSC-Grenoble [11] based on a scaler ASIC developed there. Functionally they are used as latching scalers in this application. Data are accumulated for the duration of an MPS ($\frac{1}{30}$ of a second) during which the beam helicity is fixed. Data taking is then halted by disabling the clock trains during the 500 μs helicity-stabilization period. During this break between two MPS periods, the scaler data are latched into on-board memory in the scaler modules and the scalers are then cleared. Readout of

15

the stored data via VME may then proceed, even after the next MPS has begun, since readout of the stored values does not affect the accumulation of data by the scalers.

5.3 Systematics Control Features

The data-input latch is reset at the end of any clock train during which it was set. A more deterministic deadtime is achieved by using the NPN technique of disabling data from that channel during the next beam pulse. This is done by holding the reset, preventing the latch from being set, throughout the next clock train. Thus a calculable deadtime is associated with all recorded hits. Because the enforced deadtime is longer than that of the PMTs, discriminators or meantimers, the resulting deadtime correction factor is independent of the less well-defined recovery times of those devices. Additional conventional dead-time correction factors are required, however, for events that fire only some of the four discriminators required to set the data-input latch. Those "singles" corrections have a dependence on the deadtime of the discriminators.

The effects of these deadtime corrections are demonstrated in figure 6. This shows results from dedicated test running in which a charge asymmetry, A_Q was intentionally imposed to give different beam intensity (differing by a few thousand ppm) for the different helicities. Yields are corrected to first order for beam-charge variation by dividing the observed number of detected counts by the integrated beam charge measured in the corresponding MPS. A residual yield-asymmetry, A, will be observed if the variation in deadtime loss is not properly accounted for. Since yield asymmetry is expected to be proportional to the charge asymmetry, to first order, figure 6 shows the observed slope, $\Delta A/\Delta A_Q$.

In the absence of any deadtime correction, the raw elastic-peak yield asymmetry is seen to be about 10% of the applied charge asymmetry. Correcting for the deterministic deadtime, based only upon the measured number of counts in bins of the time spectra, reduces this effect by about half. FastBus data were used to determine the rates of all possible types of partial events. These 'singles rates' included events such as a single-CFD, a single meantimer, or any possible combinations. Correction for deadtime due to these singles rates was based upon estimated effective deadtimes, taking into account the 32 ns structure of the beam. These corrections are seen to properly account for the remaining deadtime effect at the 1% level except in the last detectors. Subsequent, unpublished analysis showed that somewhat superior parameterizations of the singles deadtime could be obtained by Monte Carlo simulation of the electronics chain, but the results shown in figure 6 were those used in the published analysis of the data [3]. Linear regression analysis, applied to
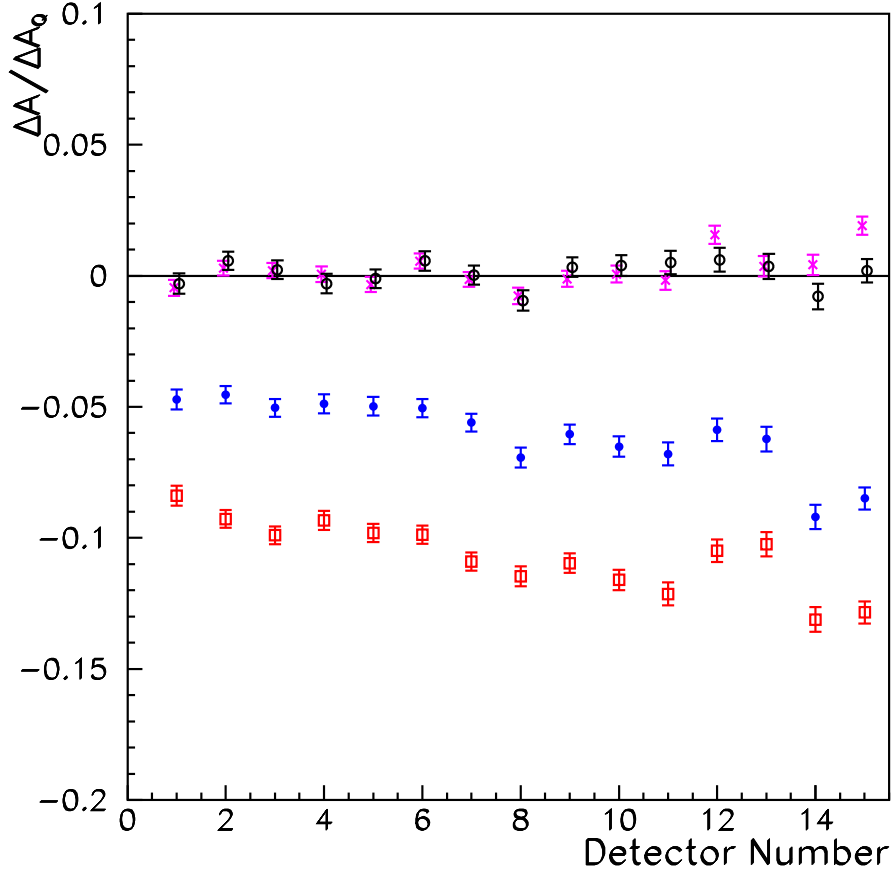
Fig. 6. Measured slopes are shown for ratio of elastic-peak yield asymmetry (A) to charge asymmetry (A_Q) (for test data taken with deliberately large A_Q). Slopes are shown for raw yields (square), yields corrected for deadtime imposed by time encoding board (solid circle), yields corrected for this and for deadtime due to singles (X), and yields with additional corrections from linear regression analysis (hollow circle).

the main data set, determined the residual dependencies of counting rates on beam parameters. Application of those corrections to this test data set is seen to reduce the yield asymmetry to less than 1% of the charge asymmetry for all detectors. Since the actual charge asymmetry during data taking was typically less than 1 ppm, the residual yield asymmetries, after these corrections, were negligible.

Each LTD board has two separate data-input latches and encodes time-of-flight for two separate FPDs, known as a buddy pair. The signal distribution was chosen so that each LTD board encodes the time-of-flight for two corresponding diametrically opposite detector pairs. That is, the signals from any

17

detector pair in octant one go to the same LTD as do the signals from the same detector pair in octant five while signals from octants three and seven are similarly paired. Separate scalers then kept track of how often a good hit occurred for each detector while its buddy was busy, as indicated by the status of the buddy's data-input latch. This gives a rough estimate of the number of events that each LTD channel missed because it was busy, itself, when a good hit would otherwise have been counted. Separate counts were kept for the number of times a hit was recorded when the buddy was busy because of a hit in the previous beam pulse and of the number of times a hit was recorded when the buddy also recorded a hit in the same beam pulse. Since coincidences are quadratic in the rates, they are expected to have the same dependence on instantaneous beam intensity as do deadtime losses. A helicity-correlated difference in buddy rates would indicate a helicity-correlated structure to beam intensity. If such a helicity-correlated intensity structure went undetected it could cause a false asymmetry by causing unexpected helicity-correlation in the actual deadtime losses which would not be compensated by deadtime corrections based on mean rates. Analysis of the buddy scalers found that most runs showed no indication of helicity-correlated intensity fluctuations, beyond the expected statistical error. A few runs, which showed large correlations, were excluded from analysis.

6 French Time-Encoding Electronics

The French electronics is fully integrated and is therefore very compact. All the required functionalities (CFDs, MTs, coincidence logic, time encoding and histogramming) are implemented on one single module processing 32 PMT signals. This module is referred to as DMCH-16X which stands for Discriminators, Meantimers, time enCoding, Histogramming, 16 MT channels within vXi standard. Thus, the 256 PMT signals from the four French octants are processed using eight modules fitting in one C size VXI crate. This crate is adapted for the 650W of power dissipated by the modules.

An additional module, called Interface Box (IB), provides common signals such as Y_0 and MPS to the eight DMCH boards through the VXI back-plane.

6.1 Interface Box

The Interface Box (IB) is a custom VXI device designed at IPN Orsay which controls all the DMCH-16X modules by means of 13 bus lines on the backplane avoiding cabling on module front panels. The IB is controlled through Device Dependent Registers. During the experiment the IB provides external signals (Y_0, MPS, 120 Hz) coming from the accelerator and the DAQ system

18

to the DMCH-16X modules. Under the control of the Trigger Supervisor the IB enables the data collection. For test purposes of the French TEE subsystem only, independently from the Trigger Supervisor, the IB generates its own simulated signals (Y_0, MPS, 120 Hz) with accurate timing from a 31.2 MHz internal crystal oscillator using an internal sequencer. The Interface Box also makes available on its front panel an internal generator signal synchronized to the Y_0 signal, to be used to test the Constant Fraction Discriminators and the meantimers of the DMCH-16X modules.

6.2   DMCH-16X mother board

Each DMCH module processes 32 PMT signals issued from eight detectors. The front-end electronics consists of 16 daughter boards, each holding two Constant Fraction Discriminators (CFDs) and one meantimer (MT), both of analog design. The CFD-MT daughter board is discussed in section 6.2.1 as is the additional generator daughter board used to internally test the CFDs and MTs. As shown in figure 7, the inputs of the CFDs are the right and the left PMT signals of each scintillator. Each MT signal corresponds to a front or a back scintillator. To reduce time differences due to signal transit time inside the electronics circuit, the front and the back channels of any one detector are implemented next to each other. The coincidence between the front and back MT signals as well as other functions, such as the buddy features ('buddy' or 'differential buddy') are implemented in an EPLD-Trig (Electrically Programmable Logic Device for Triggering) chip. Each chip handles one detector and its buddy detector (four MT channels).

In total there are four EPLD-Trig chips on each DMCH board to treat four detectors from two octants symmetrical to each other at 180 degrees w.r.t. the beam axis. The coincidence window width was set to 7 ns. The opening of the coincidence window is driven by the arrival of an MT signal from the back scintillator. For that purpose the front PMT signal was delayed by 17 ns by increasing the length of the signal cables. In case of a front-back coincidence event the arrival time of the MT front signal is tagged by the fast digital Time Encoder (TE) relative to the Y_0 beam pick-off signal. The principle of this TE will be described in section 6.2.4. One of the main advantages of this TE, when compared to the 1 ns NA electronics, is its time resolution of 250 ps which makes the background subtraction easier. As each TE holds eight channels available to flash the time, two TEs sit on a DMCH mother board implying a symmetry that can be seen in figures 7 and 8.

The event-time information from each TE is transferred to one of the two DSPs associated with the TE using asynchronous FIFOs (2048 words), see the DMCH architecture presented in figure 7. Each DSP builds two Time-
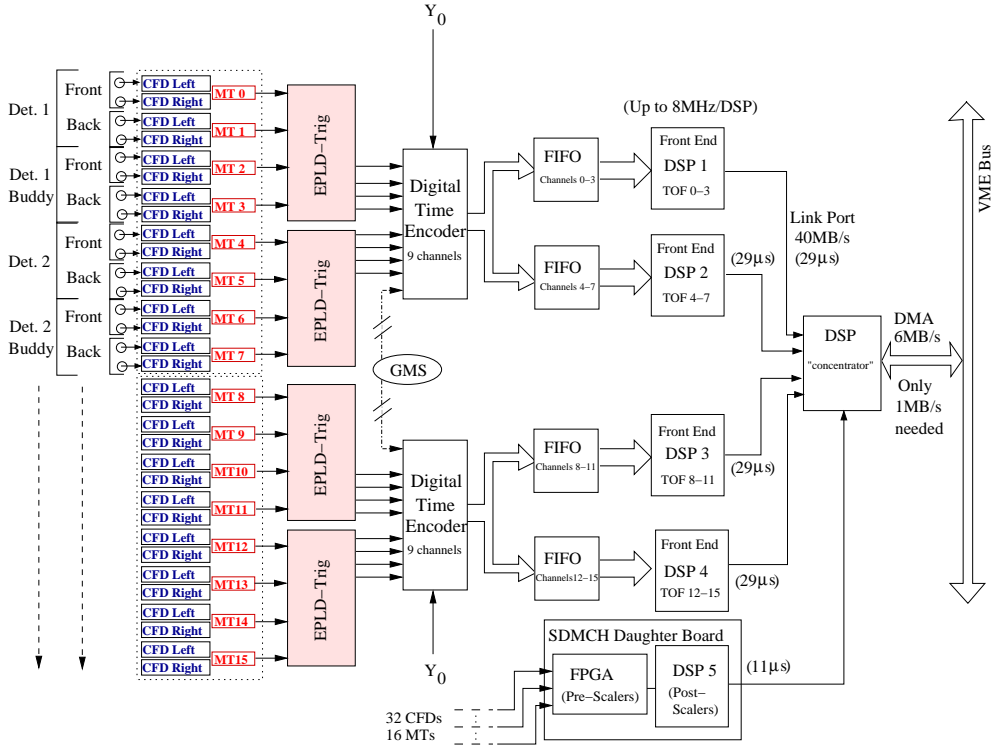
Fig. 7. DMCH architecture. The DMCH-16X mother board processes 32 PMT signals corresponding to eight pairs of scintillators. The scaler daughter board (S-DMCH) holds one FPGA (Field Programmable Gate Array) chip (104 scalers) and one Digital Signal Processor (DSP). To handle the 256 PMT signals of the four French octants, eight boards are required.

of-Flight (ToF) histograms from coincidence hits collected during one MPS corresponding to two detectors (one detector and its buddy). Each such spectrum has a fixed length of 256 Bytes. An example ToF spectrum is presented in figure 9.

Histograms stored in the four Front-End (FE) DSPs (ADSP-21062 SHARC) are then transferred to a DSP concentrator (ADSP-21062 SHARC) after the end of each MPS. One of the main challenges was to be able to build ToF spectra at such a high rate and to transfer them from the four FE DSPs to the DSP concentrator after the end of an MPS during the helicity-stabilization period. This has been achieved by using the chosen type of DSP which handles 40 MIPS and which has 2 Mbit of on-chip memory. The code of the FE DSPs has been optimized so that in only four instructions (five cycles of 25 ns) one bin is incremented. Therefore the maximum rate one FE DSP can handle is 8 MHz (4 MHz per detector). Before the transmission of ToF spectra to the DSP concentrator, 66 kbit of memory is used per FE DSP to store all the different spectra. The fast transfer from the FE DSPs to the DSP concentrator relies on link ports (40MB/s) which work in parallel. This transfer takes 29 μs.
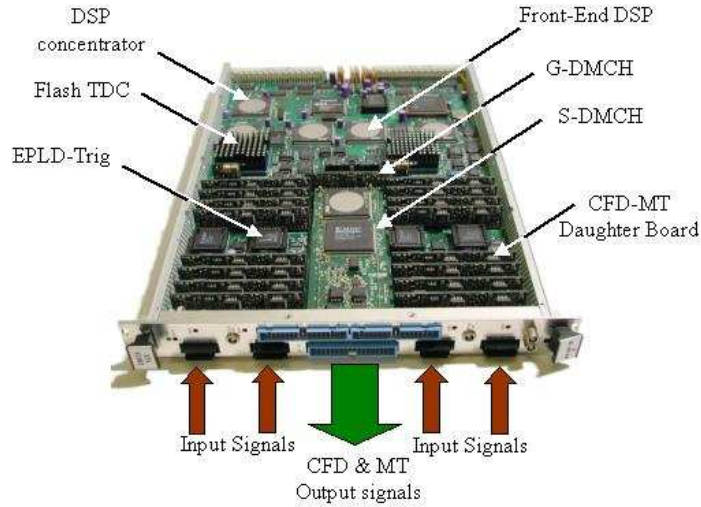
20

Fig. 8. Opened view of the DMCH-16X mother Board with its three types of daughter boards (CFD-MT, G-DMCH and S-DMCH holding a FPGA chip and a DSP) and its main components: four EPLD-Trig, two digital time encoders (flash TDC), four front-end DSPs and one DSP concentrator.

Besides the time encoding system, each DMCH board holds a daughter board, referred to as an S-DMCH (S- standing for Scalers), consisting of one FPGA chip and a DSP (see section 6.2.3). This DSP collects, for each MPS, the number of counts in each CFD and MT. In total 104 scalers are accessible. As for the four front-end DSPs, the data from the S-DMCH DSP are transferred to the DSP concentrator at the end of each MPS. The data transfer (1264 words of four Bytes per DMCH module per MPS) to the Read Out Controller (ROC) occurs during the next MPS by Direct Memory Access (DMA). At a rate of 6 MB/s, it takes 16 ms. From the ROC all the DMCH data are then gathered with the data from the other ROCs in the event builder. The total rate of the French data is 1.4 MByte/s (46 kByte/MPS) which represents 2/3 of the total G^0 data transfer.

From the CFD-MT to the fast TE, all the circuits use ECL technology whereas the DSPs, the FIFOs and the VXI management are based on MOS technology.

6.2.1 CFD-MT Daughter board:

The CFD-MT daughter board holds two analog constant fraction discriminators, a coincidence circuit and an analog meantimer whose output delay is
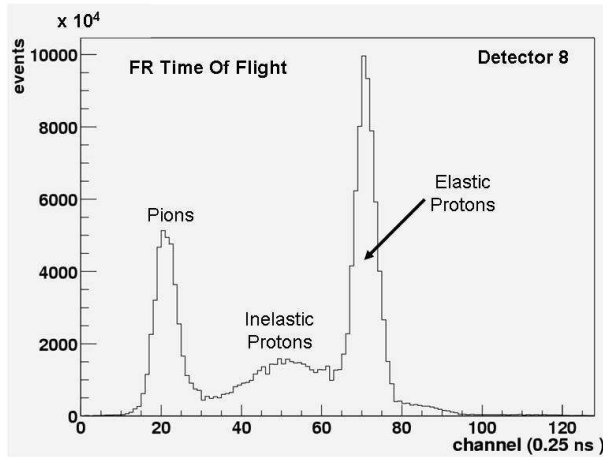
Fig. 9. Resulting time-of-flight spectrum for Detector eight (middle of the focal plane) built by the FR electronics (128 time bins of 250 ps). This ToF spectrum corresponds to an accumulation of 18274 MPS (10 minutes of data taking)

.

software-adjustable. The two discriminators accept the analog pulses from the photomultiplier bases. The advantage of constant fraction discriminators is that the firing time is independent of the amplitude of the input signals. Due to the necessity of space-saving to fit within a VXI module, a pulse shaping, integration-differentiation type CFD, using small volume L, R, C components has been chosen instead of the usual bulky delay-lines. This shaping allows the CFD input impedance to be purely resistive, not frequency dependent, provided the condition RC=L/R is achieved. A good quality 50 Ω termination is obtained for the long PMT signal cables. The schematic of this type of CFD is presented in figure 10.

The cross-talk between two adjacent channels has been measured. For an input signal of 3 ns rise time and 1 V pulse height, the cross-talk is -55 dB corresponding to an induced signal of 1.5 mV in the adjacent channel. The CFD thresholds are software-selectable from 0 mV to 255 mV (in 1 mV steps). During G^0 runs the CFD thresholds were set to 50 mV. It has been shown, using a simulation, that no pile-up effect could be observed under the conditions of G^0.

After an input signal, the discriminator is disabled until the end of the mean-timing sequence. If only one CFD pulse (left or right) is present during the MT compensation range, the sequence is reset. The MT compensation range, chosen to match the maximum transit time associated with the longest scintillator paddle has been set to 17 ns, by the value of the capacitor used. The schematics of the meantimer and its principle of operation are described re-
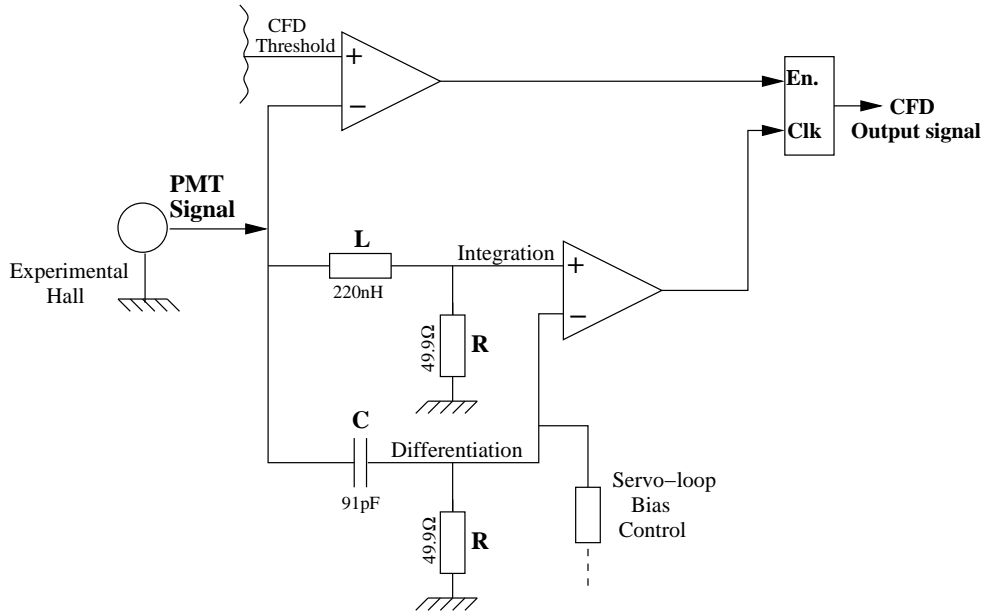
22

Fig. 10. CFD schematics.
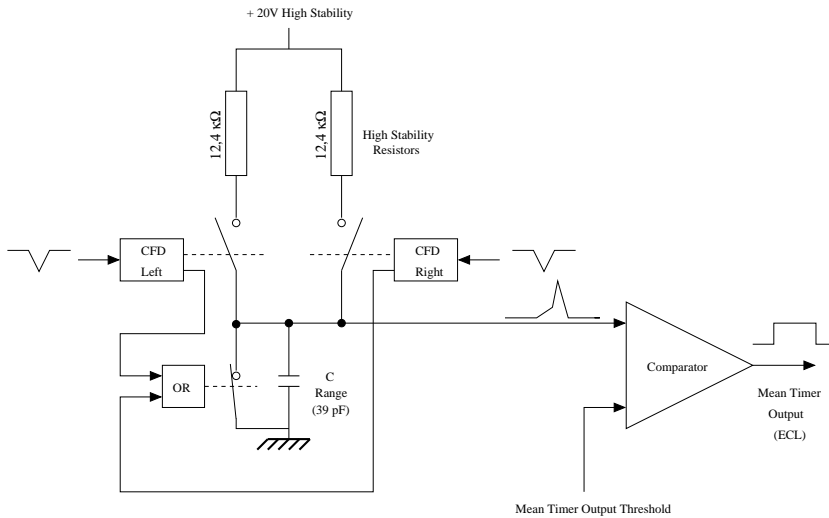
spectively in figures 11 and 12.

Fig. 11. Schematics of the meantimer (waiting state).

The MT is based on a principle which has been used at CERN since the 1960's but the design and implementation originates from the electronics department of IPN Orsay. Once either discriminator is fired, a capacitor is linearly charged with a constant current, when the second CFD fires a second equal current is added so as to make the voltage slope twice as fast. An output signal is generated as soon as the output threshold is reached. This output threshold, corresponding to the MT output delay, is adjusted by software and is mainly used to tune the coincidence between the front and the back signals. The MT output delay can be set from 0 to 44 ns in 0.175 ps steps. To avoid any time distortion on the front MT signal, only the back MT output delay has been
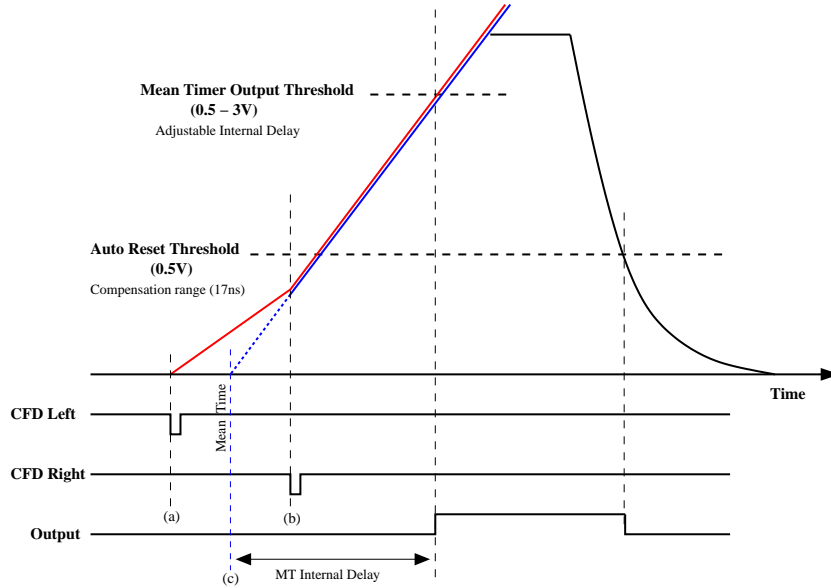
Fig. 12. MT Principle.

adjusted while the front PMT signals have been delayed by 17 ns in hardware. If only one discriminator gets a signal, then the meantimer is reset after the charge reaches the MT auto reset threshold. The MT deadtime associated with a complete MT event (two CFD pulses within the compensation range) is of the order of 37 ns depending on the setting of the back MT output delay. If only one discriminator gets a pulse then the associated MT dead time is increased to 40 ns because the MT reset occurs after the fixed compensation range. The stability versus temperature of the meantime depends only on the stability of two resistors and on the capacitor used for the compensation range. Since low temperature-coefficient components are used, the resulting drift is expected to be in the range of a few ps/°C. The cross-influence between two adjacent MT channels results in a 60 ps shift.

6.2.2 Internal Generator Daughter Board

The G(enerator)-DMCH is a custom generator designed to test the function of the discriminators and meantimers circuits. It is implemented on an additional daughter board plugged onto each DMCH-16X mother board. The G-DMCH provides two output signals simulating the left and the right PMT signals. The separation in time between the two pulses varies from 0 to the maximum time difference (17ns) corresponding to the total length of the longest scintillator. Furthermore, the amplitudes of the two pulses are software adjustable to check the discriminator threshold values.

24

6.2.3 Scaler Daughter Board (S-DMCH):

In the original design of the DMCH-16X module, this daughter board held only the 32 CFD outputs to make them available on the front panel of the DMCH module to be sent to the FastBus TDCs. Soon, it became apparent that it was very important to be able to quantify individually the number of CFD and MT signals in order to ease the evaluation of the dead time, particularly that associated with incomplete events (less than four CFD signals per detector). As the surface of the S-DMCH daughter board was fixed, it was decided to use a system of pre- and post-scalers, as described below.

For each MPS, the total number of events in each of the 32 CFDs and the 16 MTs is recorded independently of the arrival time of a hit and the completeness of the event (coincidence MT front-back). Moreover to get time information of the CFD and MT signals, a sliding time gate is used to count the number of CFDs and MTs occurring within a 2 ns time bin for each MPS. This 2 ns time window slides by 2 ns at each MPS to scan the entire 32 ns period used to build ToF spectra. The last eight scalers are the 'buddies' explained in section 4.2. The CFD and MT scalers from S-DMCH are complementary to the FastBus system and have been very useful in evaluating the dead time arising from events corresponding to only one CFD or one MT.

The 104 scalers are implemented using two chips: a FPGA (XILINX) supplying 104 pre-scalers (seven bit) and a DSP (ADSP-21062 SHARC). The DSP supplies 104 post-scalers, each of them being incremented by 127 at each overflow of the corresponding pre-scaler. In fact, once a pre-scaler reaches 127, it overflows and its corresponding carry bit is set to one. The pre-scaler itself is reset and keeps on counting. The DSP loops over the 104 pre-scaler in 23.5 μs to look for carry bits which are set to one. At the end of each MPS, the DSP reads the carry bit and the remainder of each pre-scaler and transfers the content of the 104 post-scalers to the DSP concentrator implemented on the DMCH mother board. As each pre-scaler has only seven bits for counting and a carry bit, it might happen that a pre-scaler, especially the ones corresponding to CFDs, overflows over 255 (carry bit already set to 1) before being read by the DSP. To keep track of such possible overflows, each pre-scaler has an extra bit referred to as the overflow bit. When the S-DMCH DSP reads a pre-scaler, if the carry bit and the overflow bit are set to one, then the DSP increments one specific memory location. At the end of each MPS, only the total number of overflows per S-DMCH is known. As it is not possible to correlate the overflows with individual pre-scalers, no correction can be made on the event counting over 255 but this global information has been used as an overall alert which was very useful to detect any variation in the event rates because in normal beam conditions no overflows occur. Therefore, in the off-line analysis, any quartets for which one or more alerts were found were discarded.

For the G^0 experiment, which is based on time-of-flight measurements, the time encoder is the central component as it provides the arrival time of an event. The best achievable time resolution is advantageous to achieve better background subtraction. In the French design, the digital multichannel time encoder provides time bins of 250 ps. This was designed by the electronics department of the Institute of Nuclear Physics in Orsay (France). Independently from G^0 requirements, the motivation for the design and the development of this ASIC, based on 1.2μ ECL bipolar prediffused technology, started in 1990 to provide a generic tool for nuclear physics experiments relying on accurate time measurements. This TE has nine independent channels. The ninth channel, which serves as a start signal wasn't used for G^0. Instead, the start for the eight channels is given by a Voltage Controlled Oscillator (VCO) locked on the Y_0 reference signal. Consequently, the encoded time corresponds directly to the ToF without any calculation. The possibility of using this mode for G^0 is one of the main features of the time encoder which, coupled to FIFOs and front-end DSPs, allow us to build ToF spectra at a rate of 4 MHz per detector.

The principle of the time encoding is very classical. Fundamentally, the TDC is made of a crystal oscillator, delivering a period T (here $\approx$ 4 ns), a 'standard' counter running at the frequency $\frac{1}{T}$ for counting of the periods and a 'fast' counter, slicing the period T (interpolation). The standard counter runs continuously. The fast counter relies on Delay Locked Loop (DLL) circuits which split the period of the standard counter into sixteen time slices of $\approx$ 250 ps representing the time bins, see figure 13. The frequency of the standard counter is provided by a VCO (figure 14). This frequency f_{VCO} divided by 64 is locked on an external frequency f_{ext}. In the case of the G^0 experiment, the external frequency is the Y_0 signal of 31.1875 MHz divided-down by eight to match with f_{VCO} / 64. This comparison is made by a Phase Locked Loop (PLL) which generates a proportional error voltage to continuously adjust the VCO frequency to the external frequency.

The total width of the first eight time slices is locked to half of the VCO period, see figure 13. As the width of each individual time slice is not locked and because the transit time from one transistor to another can differ, a time differential non-linearity from bin to bin can be observed.

According to the scheme presented in figure 14, the encoded time results from a fine and a coarse time code. The fine time code (0 through 15) given by the period-slicing corresponds to the time within one period ($\approx$ 4 ns). This fast counter is a Johnson-type counter requiring only one bit to change at a time. The coarse time code provided by the standard counter tells us in which period the event occurred among the eight periods required to get the Y_0 period. This standard counter is a natural-progression binary type.
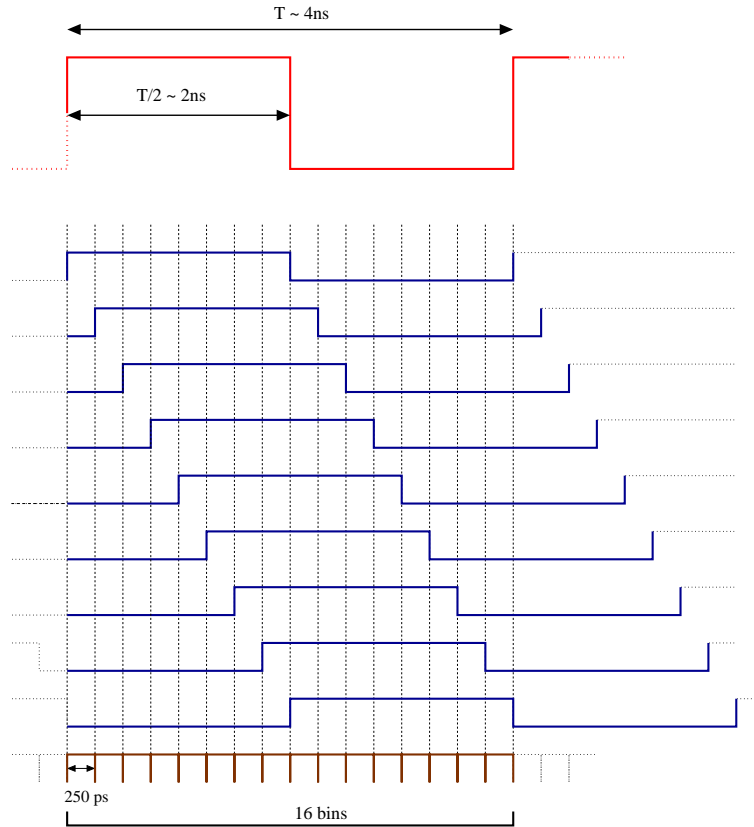
Fig. 13. Basic principle of the period slicing using the reference signal ($\approx$ 4ns) using eight Delay Locked Loop (DLL) circuits.

In the design of such a Time Encoder, three issues require special care. First, as the arrival of the physics event is asynchronous with the internal frequency of the Time Encoder, care must be taken to ensure that the time code is unambiguous when the latch of the fast counter occurs. This has been solved by using a Johnson type counter. Second, the standard counter being a conventional binary counter driven by the internal frequency of the Time Encoder, has to be latched when its contents are stable. To achieve this requirement, the triggering of the latch of the standard counter is delayed with respect to the internal frequency of the Time Encoder such that it occurs in a time window in which all the bits are stable. Lastly, the standard counter code has to be correctly aligned with the code provided by the fast counter. In practice, it is impossible to increment the standard counter exactly in coincidence with the roll-over of the fast one. Because the triggering of the latch of the standard counter cannot be perfectly synchronized with the latch of the fast counter, an error of one period T could occur. This error is corrected by means of a supplementary 'corrector' bit which stores the value of the least significant bit of the standard counter at the middle of the period of the fast counter. When the standard counter is latched, the value of its least significant bit is compared to the corrector bit and a table is used to determine whether a correction of the least significant bit is to be made within the ASIC itself.
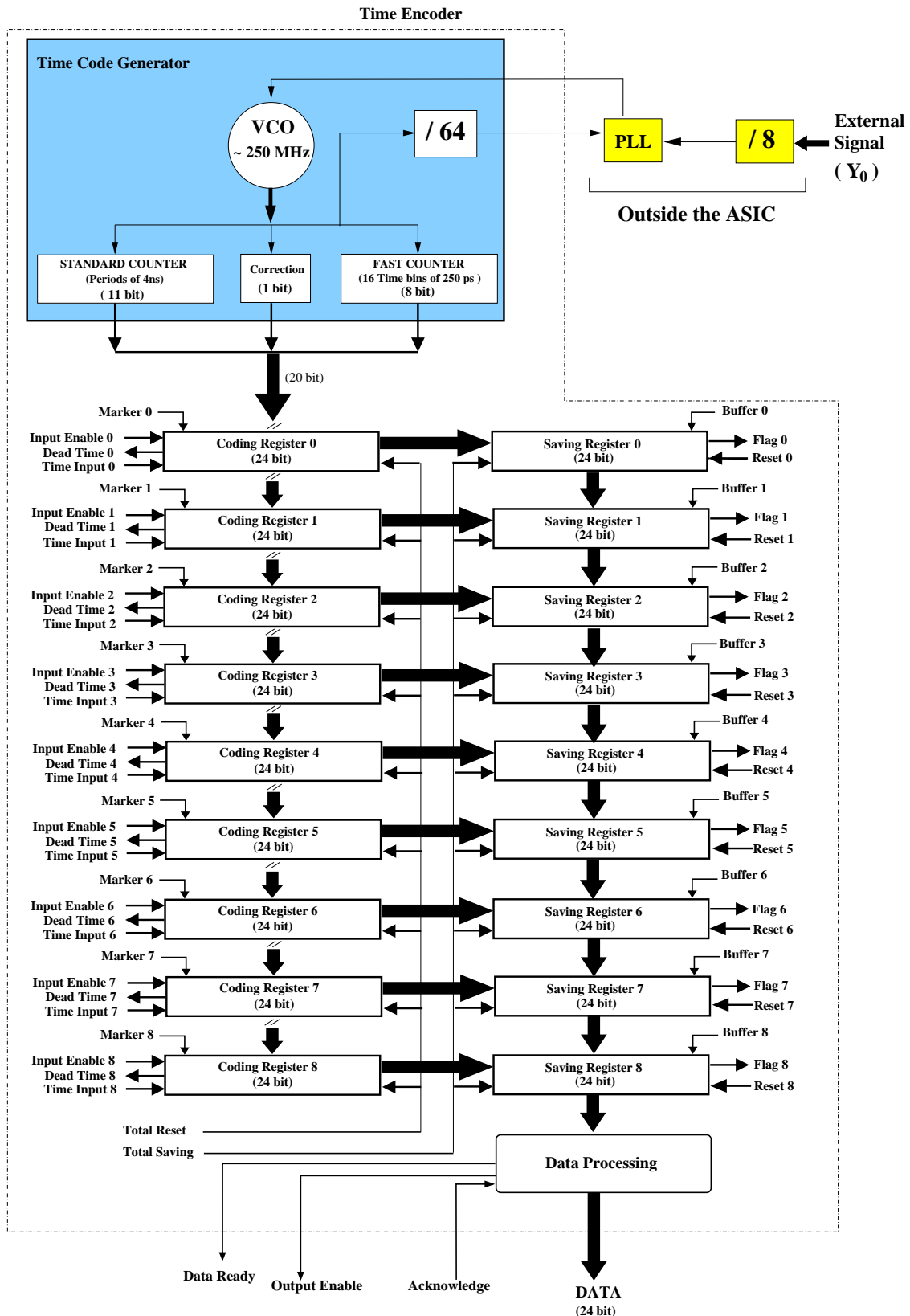
27

Fig. 14. Internal architecture of the Time Encoder. The nine inputs to coding registers are independent channels. As indicated, the external Phase-Locked Loop (PLL) adjusts the internal Voltage Controlled Oscillator (VCO) to synchonize it to the Y_0 signal.

Once an event occurs in any of the eight channels of the TE, the contents of the two counters are latched into the corresponding coding register. The nine coding registers are independent of each other. Each coding register is linked with a saving register in order to quickly release the coding register, lowering the coding dead time (24 ns). The coding registers are arranged in a synchronous FIFO architecture to buffer a possible burst of input signals as well as to multiplex and send the coding results.

The intrinsic dead time of the Time Encoder is of the order of 24 ns. Compared to the 37 ns of dead time associated with the meantimers, the TE does not add any extra dead time.

Intrinsically, the time encoder presents a Differential Non Linearity (DNL) from bin to bin which is very sensitive to temperature variations. For a given temperature of operation, the DNL of the time encoder can be minimized by software. As the DNL acts on the bin width, an off-line correction has to be applied to allow correct extraction of the events associated with the different Q^2 from the same detector (as occurs for detectors 14 and 15 of each octant, as explained in section 2.3). Periodically, in the absence of beam, background data were taken using a radioactive source. Ideally, for long data-taking with no DNL effect, we would expect flat time-of-flight spectra. In fact, without beam, the deviations seen in the ToF spectra compared to a flat spectrum are a measure of the differential non linearity of the time encoder. Relying on the background ToF spectra, the width of each bin is adjusted by software and a corrector factor is applied to the ToF obtained with beam. More details on the principle of this correction can be found in reference [12].

Independent of the DNL, the ToF spectra present a bin-to-bin correlation. This effect has been well reproduced by a simulation (Appendix A of reference [6]) which indicated a jitter of 50ps modulated at 1 to 10 kHz. This jitter is strongly suggested to originate from electronic noise (voltage control of the TE, etc.) surrounding the DLL circuits which build the time bins at the level of the fast counter. This effect is amplified by the implicit mode of operation chosen for G^0. The global systematic uncertainty due to the bin-to-bin correlation has been estimated to 0.025 ppm.

6.3 Dead Time corrections

One significant issue for the G^0 experiment is the ability to deal with the dead-time of the electronics. If associated with beam charge asymmetries and/or detector counting asymmetries for time ranges outside of the one of interest, the deadtime could induce sizeable asymmetries on the elastic counting rates. The resulting systematic error on the asymmetries, which is proportional to

the deadtime itself, will then be minimized by correcting for the deadtime losses as well as possible. It is then important to know the precision that can be achieved for deadtime corrections.

As discussed above the deadtime is due to the front-end electronics, upstream of the time encoding system, consisting of the discriminators (CFD) and meantimers (MT). Also to improve the accuracy of the correction, the Next Pulse Neutralization (NPN) procedure has been implemented, meaning that the deadtime is extended precisely up to the end of the next 32 ns time window, for coincidences between the front and back meantimers.

Due to the beam time structure, the deadtime correction, to be applied to the measured counting rates before calculating the asymmetries, must be estimated bin by bin over the 32 ns time spectra. This consists of two main contributions. The first is due to the probability for having a preceding coincidence between the back and the front detectors, which prevents encoding of an event at bin i (32 ns corresponds to 128 bins of 250 ps width). This probability can be determined directly from the time-of-flight spectra provided by the DMCH16X, including the effect of the NPN system. The second contribution to the deadtime, is due to the probability for one single meantimer (front or back) or one of the four discriminators being fired, which can prevent a subsequent front-back coincidence from being encoded. The time distributions associated with single CFDs or MTs are obtained from the analysis of the FastBus data, which also allows proper accounting for all possible configurations, such as firing of two CFDs which are not associated with the same meantimer or firing of one meantimer in coincidence with one single CFD. As discussed in section 6.2.1, the deadtime due to the meantimer itself, differs when only one or both CFDs fire(s) on the same meantimer. The deadtime correction was calculated by taking into acount the appropriate deadtime for each of the different configurations with the normalization being provided by the individual scalers of all CFDs and meantimers implemented on the daughter board S-DMCH.

A number of studies have been carried out to check the ability to accurately correct for deadtime losses.

A first test, dedicated to the deadtime correction due to front-back coincidences, used a high intensity Strontium source coupled to a PMT, allowing counting rates up to 4 MHz. The time distribution of the measured coincidences, relative to an arbitrary 32 ns time window, depends upon the time bin due to the NPN system, with the slope of the time distribution being directly proportional to the deadtime itself. This test demonstrated [13] that deadtime corrections, involving only coincidence events, can be predicted with a precision of about 1%.

A second test was carried out in the G^0 beam conditions, where the deadtime losses due to single CFDs and MTs were comparable to those from front-back coincidences [12]. Measurements were performed with several beam currents up to 40 μA [14]. The slope of the yield (normalized to the beam charge), against the beam current is expected to be proportional to the deadtime. This slope can be extracted before and after applying deadtime corrections and is used to estimate the precision of the correction. Figure 15 shows this slope normalized by the yield, itself, (in % /μA) for each detector. This has been multiplied by the beam current to obtain the corresponding deadtime. It can be seen that the deadtime at the nominal beam current of 40 μA ranges between 8 and 16%. Application of the deadtime corrections due to single CFDs, single MT and coincidences reduces the beam current dependency to a residual deadtime of 1 to 4% for the French detectors.
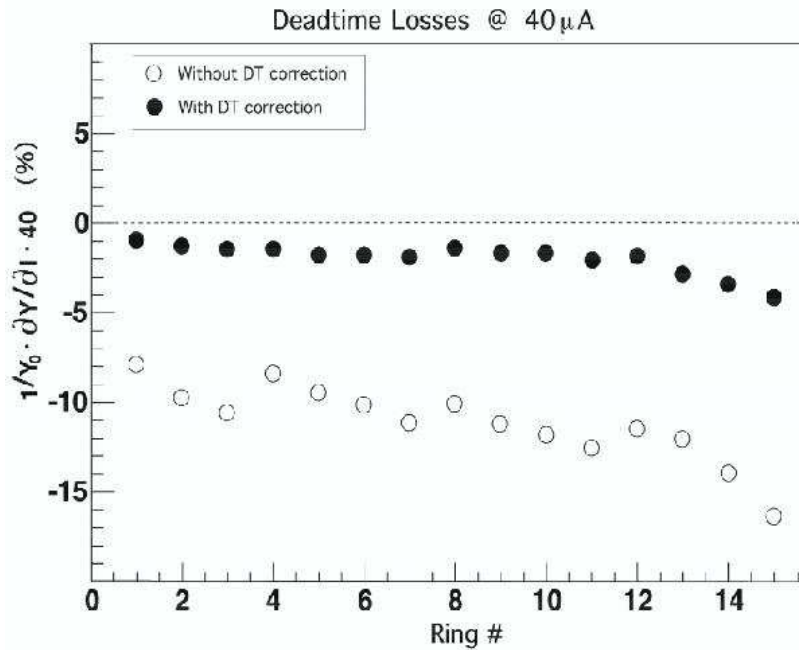

Fig. 15. Residual deadtime obtained from the dependence of the normalized yield on beam current. Here the observed effect of deadtime is plotted before and after deadtime correction for the French octants.

Another study was performed by analyzing the detector yield asymmetry as a function of the beam charge asymmetry [14]. For this test, dedicated runs were recorded with charge asymmetry varying between -4000 and +2000 ppm, imposed by a Pockels cell device at the electron source. The slope of the detector yield asymmetry versus the beam charge asymmetry is directly proportional to deadtime. Figure 16 shows the results obtained at 40 μA, which are in agreement the previous ones obtained by varying the beam current between 0 and 40 μA.

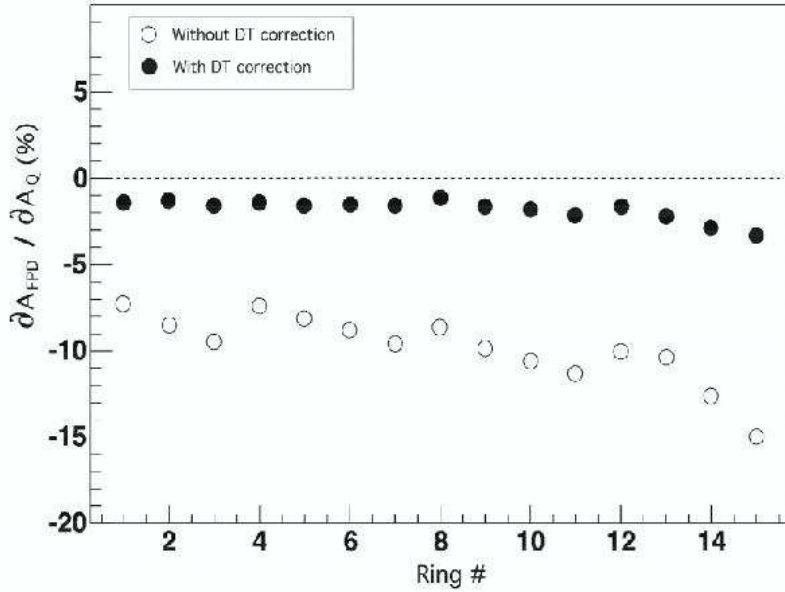In conclusion, the studies performed on the French electronics have shown

Fig. 16. Residual deadtime obtained from the dependence of the detector yield asymmetry as a function of beam charge asymmetry for different deadtime corrections. Here the deadtime is plotted before and after deadtime correction for the French octants. Linear regression analysis is not included.

that we were able, in realistic conditions, to estimate about 80 to 90% of the deadtime using an analytical approach without any free parameters. The remaining dependence of the counting rates on the beam current was removed using a linear regression analysis.

7 Summary

The forward-angle part of the G^0 experiment required the equipment described here to permit the extraction of the elastic-scattering asymmetry. This part of the experiment has been successfully carried out and the results of the analysis have been presented in reference [3]. That analysis combined the results from all octants of the spectrometer. Figure 17 shows the elastic asymmetries, as extracted detector-by-detector, separately for the four octants instrumented with French electronics and detectors and for the four octants instrumented with North American electronics and detectors. These asymmetries are extracted, for each detector, by correcting for background contamination, as described in reference [3].

No evidence is seen of a systematic difference when the results obtained with one set of equipment are compared to the other. Despite significant differences in design and operation, the results from the two sets of apparatus are seen to
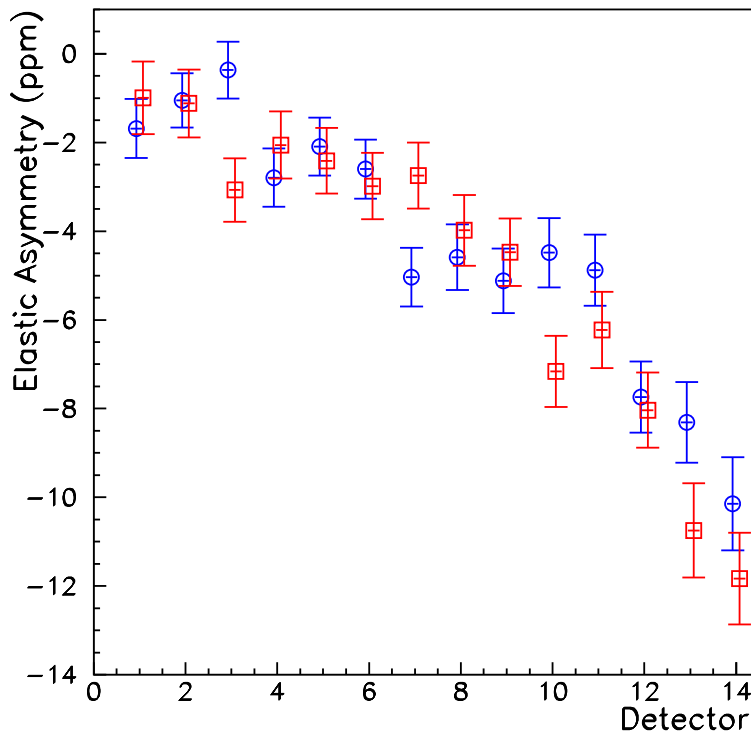
32

Fig. 17. Elastic asymmetries, detector-by-detector, as measured using only the four octants instrumented with North American apparatus (circles) or the four octants instrumented with French apparatus (squares). Error bars represent statistical errors. Data points have been slightly displaced horizontally to aid in comparison.

be in excellent agreement. This serves to strengthen confidence that neither set of apparatus has introduced unintended systematic distortion of the data.

8   Acknowledgments

33

lems. We would like also to acknowledge the technical staff from LPSC which have contributed to the DAQ and electronics implementation : G. Barbier, G. Bosson, D. Dzahini, J.P. Girard, S. Muggeo, J.P. Scordilis.

References

[1] P. G. Roos et al., "The G0 experiment: Parity violation in e-N elastic scattering", Eur. Phys. J. A24-s2 (2005) 59, Proceedings of PAVI04 international workshop (Grenoble, France).

[2] D.S. Armstrong et al., (The G^0 collaboration), "Apparatus for the G^0 experiment", NIM, to be published.

[3] D.S. Armstrong et al, "Strange Quark Contributions to Parity-Violating Asymmetries in the Forward G0 Electron-Proton Scattering Experiment", Phys. Rev. Lett. 95, 092001 (2005).

[4] J. Musson, T. Allison, A. Freyberger, J. Kuhn, and B. Quinn, Nucl. Inst. Meth. A 540, 448 (2005).

[5] S. D. Covrig et al., "The Cryogenic Target for the G^0 Experiment at Jefferson Lab. The G^0 target", Nucl. Instrum. Meth. A551 (2005) 218, arXiv:nucl-ex/0502019 .

[6] S. D. Covrig, "A measurement of parity-violating asymmetries in the G0 experiment in forward mode", PhD Thesis (09/28/2004), California Institute of Technology, URN etd-12222004-075215.

[7] S. E. Williamson et al., "Performance of the G0 superconducting magnet system", Eur. Phys. J. A24-s2 (2005) 143, Proceedings of PAVI04 international workshop (Grenoble, France).

[8] http://coda.jlab.org

[9] L. Bimbot, "A bin-per-bin dead-time control technique for time-of-flight measurements in the G0 experiment: The differential buddy", Eur. Phys. J. A24-s2 (2005) 147, Proceedings of PAVI04 international workshop (Grenoble, France).

[10] R. Foglio, J. Pouxe, O. Rossetto, "Design and Performances of a compensated meantimer", internal report G0-99-003, LPSC 99-07.

[11] J. Bouvier, R. Foglio, E. Munoz, O. Rossetto, "Scale 32", internal report G0-99-017, LPSC 99-10.

[12] G. Batigne, Thèse d'Université (LPSC 03-41), Mesure du contenu étrange du nucléon : expérience G^0, Université Joseph Fourier, Grenoble, France.

[13] J. Arvieux et al., "Deadtime corrections for French electronics", internal report G0-01-016.

[14] B. Guillon, Thèse d'Université (LPSC 05-89), "Contribution du quark étrange à la structure électromagnétique du nucléon : Les premiers résultats de l'expérience G^0", Université Joseph Fourier, Grenoble, France.